Journal of Alloys and Compounds 836 (2020) 155513

Contents lists available at ScienceDirect

Journal of Alloys and Compounds

journal homepage: http://www.elsevier.com/locate/jalcom

Interdiffusion and diffusion paths in two-phase γ+β|γ+β diffusion couples. Comparison of experimental investigation with theoretical predictions

M. Zajusz [a, *], M. Jawańska [a], J. Dąbrowa [a], K. Berent [b], M. Danielewski [a]

[a] Faculty of Materials Science and Ceramics, AGH University of Science and Technology, Al. Mickiewicza 30, 30-059, Kraków, Poland
[b] Academic Centre for Materials and Nanotechnology, AGH University of Science and Technology, al. Mickiewicza 30, 30-059, Kraków, Poland

ARTICLE INFO

Article history:
Received 17 October 2019
Received in revised form
4 May 2020
Accepted 5 May 2020
Available online 8 May 2020

Keywords:
Diffusion
Two-phase
Ni-Cr-Al
DICTRA
Simulation

ABSTRACT

The first-ever experimental results concerning the interdiffusion in the two-phase, γ+β region of the ternary system are presented, together with the theoretical interpretation of the observed phenomena. In the experimental part of the study, a number of two-phase diffusion couples made from cast Ni-Cr-Al alloys was studied at 1200 °C. The application of the novel wide-line Energy-dispersive X-ray Spectroscopy (WL-EDS) allowed for previously impossible quantitative measurements of the concentration profiles within the two-phase zones. The measured profiles, together with the determined diffusion paths, were compared to the results of the simulations performed with the use of two different models: the Engström et al. model (DICTRA) and multi-component multi-phase model. The results allowed verifying the existence of a number of previously postulated features typical for the multi-phase diffusion. The comparison of the experimental and simulated results confirms that the currently used theoretical models of the interdiffusion process enable a satisfactory description of the real process. Still, some of the observed features cannot be interpreted in the light of available theory, although some of them are likely caused by the non-uniform cast microstructures. The better agreement with the experimental data obtained with the use of multi-multi model suggests that the interdiffusion should be considered simultaneously in all phases present in the system.

1. Introduction

Despite the popularity of dual-phase alloys in commercial applications, especially as high-temperature structural materials (e.g. superalloys), relatively little is known about their diffusion behavior, which is a major limitation when it comes to their design and life-expectancy predictions. Although the first model describing the process of interdiffusion in two-phase alloys was presented by Roper and Whittle in 1981 [1], the period of the modern development in this field was started in 1994 simultaneously by Hopfe and Morral [2], and Engström et al. [3]. The first study served as a base for further works [4–6], both theoretical and experimental, which revealed a number of features distinct for a multiphase diffusion such as "zig-zag" diffusion paths and diffusion paths with "horns" [5,6], which due to the numerical artifacts in Ref. [4], were initially a source of controversies, before their further verification [5,7]. Based on the results of numerical simulations and limited experimental data [8,9], Morral et al. proposed the existence of three different interphase boundary types within the multiphase diffusion zones [10]. Later, in the works of the same team, the diffusion theorems formulated by Kirkaldy and Brown [11] were further developed to describe the phenomena which can occur only in multiphase diffusion [12]. The described studies by Morral et al., greatly increased our state of knowledge regarding the diffusion phenomena in multiphase systems. Nevertheless, it is the model by Engström et al. [3] which is perhaps the most influential one, thanks to its integration into a computational module DICTRA [13,14] and incorporation into the framework of Thermo-Calc thermodynamic and mobility databases. Consequently, as of today, this is probably the most popular and widespread description of the multiphase diffusion, which at some stages was used to verify the existence of a number of theoretical features e.g. Ref. [10].

The further development of the theoretical description of interdiffusion in multiphase alloys can be divided into two

* Corresponding author.
E-mail address: zajuszm@agh.edu.pl (M. Zajusz).

https://doi.org/10.1016/j.jallcom.2020.155513

categories. The first one is based on the phase-field method enabling a better description of microstructure evolution [15–17]. The second one focuses on the further refinement of the theoretical description of the interdiffusion process with the use of the Darken approach [18].

Unfortunately, while the theoretical developments flourished, the experimental studies lagged behind, mainly due to the limitations in the possibility of measuring the concentration profiles in the multiphase zones, which in turn hinders our ability to validate the correctness of the theoretical descriptions. The first experimental studies of multiphase diffusion couples started in 1978 in NASA Lewis Research Centre [19] but were limited just to metallographic observations of the annealed diffusion couples. Later studies provided for the first partial measurement of the concentration profiles between $\gamma+\beta$ and $\gamma+\gamma'$ regions in Ni-Cr-Al system – however, only in the single-phase zones the quality of determined concentration profiles and diffusion paths was good enough to allow interpretation of the data [20]. Further works in this field performed by Nesbitt et al. [21,22] and Merchant et al. [23,24] did not bring any breakthrough concerning the two-phase diffusion and the methodological approach to the study of this phenomenon. The first reliable measurements of the diffusion path trajectory were conducted by Xin in 1998 for Ni-Cr-Al $\gamma+\beta$ and $\gamma+\gamma'$ couples [25], similarly as in Ref. [20]. The applied approach was based on the measurement of the constituents' average concentrations in relatively big rectangular zones on the cross-section of the diffusion couple, thereby obtaining very precise results at the cost of a very poor spatial resolution. The first, and probably the only experimental data for a diffusion couple consisting of materials with initial compositions lying in the same two-phase region, were measured for a ternary Fe-Ni-Al system by Sohn et al. [26]. However, the diffusion paths presented therein greatly differed from the zig-zags predicted with the use of computational simulations. Namely, in the place of zig-zag diffusion path with 0-type interphase boundary. two single-phase zones were observed. What is more, no concentration changes were observed within the two-phase zone. It is yet to be determined whether the observed behavior was a result of differences in thermodynamics between the Fe-Ni-Al and Ni-Cr-Al systems or evidence of the incorrectness of the mathematical models used.

Recently, a few studies dedicated to multiphase diffusion zones were published. Most of the experimental works in this field benefit from the established theoretical descriptions, focusing rather on the practical aspects of diffusive interactions [27,28] or on the application of diffusion couple experiments as a way to explore the phase diagrams, e.g. Eastman et al. [29]. In this particular paper, the diffusion multi-couple experiments in Ni-Cr-Pt were performed, but the diffusion process was considered only in the single-phase zones and as a result, neither new diffusion data nor theoretical description of the process in the two-phase zone were provided. Another recent work, focusing strictly on the diffusion in the multiphase system, is the article by McGregor et al. [30]. In this study, the formation of dual-phase Ni-Al-Ta coating on the surface of superalloy was considered. However, the agreement between experimental data and results of the DICTRA simulations was rather poor. Other recent studies in the field were carried out by the team of Wierzba et al. [31–33]. However, the first two articles concern mainly the subject of the trajectory of diffusion paths determination in complex systems and predicting the phase formation, and do not provide information concerning both the concentration profiles shape and diffusion in multiphase zones. Only in the case of [33], the process of interdiffusion was treated in detail, but similarly as in Ref. [31], the analysis was limited strictly to the single-phase regions.

The main goal of the presented study is to provide the first experimental data on a comprehensive variety of diffusion paths that can occur in ternary, two-phase, diffusion couples. The current work benefits from the recently developed wide line EDS (WL-EDS) analysis [34], allowing for measuring the concentration profiles even in the multiphase zones. The experimental results are compared with the results of computational simulations performed with the use of two different models – the model of Engström et al. implemented in DICTRA [3,35], and the multi-component multiphase model proposed by Danielewski et al. [18]. Thus, it was possible to verify the existence of some of the features typical only for the diffusion in two-phase zones and the models' correctness was also tested in the process.

The Ni-Cr-Al system was chosen based on the existence of a large $\gamma+\beta$ two-phase region on the phase diagram, which greatly simplifies the experimental procedure. It is also a host system for the Ni-based superalloys and therefore has already been described in numerous papers [36–40] making it probably the best-studied ternary system. Also, considering the popularity of Ni-based superalloys, such a choice of the system brings additional, application-oriented value to the study.

To avoid ambiguity, the nomenclature proposed by Gusak [41] is used within the whole paper. According to it, areas observed on the SEM image are denoted as **zones** (single or two-phase). They are separated by **interphase boundaries**. Furthermore, the areas on phase diagram are called **regions** and they are separated by the **phase boundaries.**

2. Experimental methodology

All alloys used in the experiments were provided by the Good-Fellow Inc. in a form of cylindrical ingots of 99.99% purity. The chemical compositions of the alloys (both nominal and experimental determined from the area analysis with the use of energy-dispersive X-ray spectroscopy), symbols denoting respective end-members used through the paper, and γ-phase volume fractions, calculated for the nominal compositions with the use of the Ni-Cr-Al phase diagram [36], are specified in Table 1. As visible, the agreement between the nominal and experimental values was very good, and in most cases, the nominal compositions were taken as the end-members during simulations. All considered compositions were chosen from the Ni-rich corner of the Ni-Cr-Al ternary phase diagram, as can be seen in Fig. 1. The SEM (Scanning electron microscopy) and XRD (X-ray diffraction) characterization confirmed that, as expected, all alloys were two-phase $\gamma+\beta$-structured with chemical compositions being close to the nominal ones. To study the phase stability of the materials, some of them were initially annealed in the vacuum furnace, at 1200 °C, for the duration of 24 h. However, the only observed effect was the increase in the average grain size. Therefore, to avoid excessive grain growth of the precipitates, which would negatively impact the accuracy of the applied method of composition analysis, the further experiments

Table 1
The symbols, nominal and EDS measured compositions, and nominal volume fractions of γ-phase (at 1200 °C) for the alloys used in the experiments.

Symbols	Composition (at. %)						β-phase fraction (vol. %)
	Nominal			Measured			
	Cr	Al	Ni	Cr	Al	Ni	
1L	8	28	64	7.58	26.86	65.56	91.7
2L	11	23	66	10.53	23.55	65.92	51.3
3L	15	18	67	14.50	18.49	67.01	12.3
1R	13	29	58	12.82	28.24	58.94	94.0
2R	21	22	57	20.07	21.68	58.26	53.1
3R	30	15	55	29.75	15.74	54.50	13.4

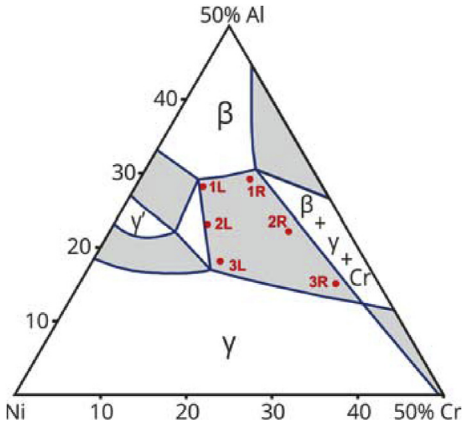

Fig. 1. The Ni-rich corner of the Ni-Cr-Al phase diagram at 1200 °C with marked nominal compositions and symbols of alloys used in the experiment. The phase diagram was drawn after CALPHAD [36]. The grey areas denote two-phase regions.

were conducted with the use of as-cast alloys.

To prepare the diffusion couples, the alloys were cut into ca. 1 mm thick slices. Then, the slices were ground and polished with the use of standard Struers procedure down to 1 μm diamond suspension and assembled into molybdenum holders. To allow following the change of the position of the Kirkendall plane, the submicron thorium dioxide particles were applied to the initial contact interfaces with the use of acetone suspension. The diffusion annealing was conducted for 24 h at 1200 °C in a rotary vacuum furnace under a high vacuum of 10^{-6} Tr provided by Pfeiffer Vacuum HiPace® 80 pump. To preserve the high-temperature phase structure intact, the annealing was finished by vacuum quenching, by removing the sample directly from the heating zone into the cold regions (<100 °C) of alumina tubing. While certainly less effective than conventional air- or liquid-quenching, it allowed for cooling the sample into the temperature range where all phase transformations are negligible due to kinetic constraints, within a few seconds.

The annealed diffusion couples were cut into halves, hot-mounted in the conductive resin, and polished using the same metallographic procedure as during experiment preparation. Then, the samples were examined with the use of SEM-EDS techniques (apparatus: FEI Versa 3D Scanning Electron Microscope equipped with EDAX Apollo XP Silicon Drift Detector). To measure average concentration in the two-phase couples the wide line EDS (Energy-dispersive X-ray spectroscopy) method was used [34]. The width of the line (the dimension in the direction parallel to the interface plane) was usually about 300 μm, however, for each couple, it was slightly adjusted in order to adapt to the observed microstructure and to optimize the quality of the results. The applied step, in the direction perpendicular to the initial interface plane, was 5 μm, with the total length of the line being adjusted for particular cases. To draw the diffusion paths, the concentration profiles were smoothed with the use of Savitzky-Golay filter [42]. The diffusion paths were compared to the phase diagram calculated by CALPHAD for the temperature of 1200 °C [36].

In the next sections of the article, only some of the most important results are presented. All measured concentration profiles, including the repeated measurements, are available in supplementary materials.

3. Simulations

In the present study, two different models of interdiffusion in multiphase systems were used and compared with the experimental results: the multi-phase, multi-component model developed by Danielewski et al. [18] and model by Engström et al., implemented within the DICTRA software [3,35].

Table 2
Average intrinsic diffusion coefficient for γ+β Ni-Cr-Al system at 1200 °C.

Phase	Diffusion coefficient $[m^2/s]$		
	Ni	Cr	Al
β	$4.8 \cdot 10^{-13}$	$3.5 \cdot 10^{-14}$	$4.6 \cdot 10^{-14}$
γ	$4.2 \cdot 10^{-13}$	$9.3 \cdot 10^{-15}$	$1.4 \cdot 10^{-13}$

The multi-phase multi-component model ("multi-multi") is based on the Darken approach to the interdiffusion. In this model, diffusion takes place in both of the existing phases and the driving force for diffusion in each of them is the respective concentration gradient. It assumes orto-equilibrium between phases calculated according to the phase diagram. The biggest advantage of the model is the assumption of diffusion occurring simultaneously within both phases. On the other hand, an assumption of the ideality of the system used to calculate driving forces and lack of data concerning the diffusion coefficients should be regarded as its drawbacks. The detailed description of the model can be found elsewhere [18].

The phase equilibria in performed multi-multi simulations were calculated according to the Ni-Cr-Al phase diagram generated by CALPHAD [36]. Due to a limited amount of literature information concerning the intrinsic diffusion coefficients in the γ-phase, the diffusion coefficients used in this paper were obtained from the Thermo-Calc database [4,43] with the use of inverse methods. The obtained values of intrinsic diffusion coefficients are listed in Table 2. The values determined for β-phase were in a very good agreement with results published by Campbell [44], confirming in the process the correctness of the applied approach. The multi-multi model was solved in 1D space with the use of the finite differences method (the Euler method), with the evolutionary time step. The spatial step was 10 μm, while the total length of the system was ascribed individually to each diffusion couple, in a way ensuring the semi-infinity of the systems. In the case of DICTRA model, the calculations were carried out with the use of the inverted Chebyschev grid, with the nodes being denser near the initial interface. The spatial step varied depending on the considered case, with the number of nodes ranging from 59 to 89, yielding a slightly bigger spatial step than in the case of multi-multi model. The applied time integration method was the backward Euler method.

As already mentioned, the model of interdiffusion implemented in DICTRA is based on the theoretical description provided by Engström et al. [3]. It also assumes the orto-equilibrium between phases. However, in this model, it is assumed that the diffusion occurs only through the matrix phase, in this particular case in the γ phase. The biggest advantage of the model is its compatibility with the thermodynamic and mobility databases provided by Thermo-Calc. It allows including the chemical potential gradients as a driving force for diffusion. The biggest disadvantage, other than the single-phase diffusion assumption, is the black-box form of the program, which does not allow full control of the input data and calculations.

The presented DICTRA simulations were conducted with the use of TCS Ni-based superalloys v.8 and TCS Ni-alloys mobility v.4 databases.

4. Results and discussion

The following section was divided into three subsections. In the

first of them, the theoretical predictions for all considered types of diffusion couples are presented, including both profiles and diffusion paths. In the second subsection, the experimental results are described, including the discussion concerning potential errors and artifacts. In the last subsection, the agreement between theory and experimental data is discussed, including a comparison of the applied models. It should be noted that while the presented approach for determining the concentration profiles is characterized by a much better spatial resolution than it has been possible until now, still the effects of the non-uniform microstructure resulting from the casting process, combined with the errors of the EDS method, may in some cases affect the quality of the results. This is especially problematic when comparing the experimental concentration profiles with the results of theoretical simulations. Therefore, the much bigger focus is put on the more reliable features of the diffusion paths.

4.1. Predicted diffusion behavior

In the presented study, three different types of diffusion couples are considered:

- Diffusion couples in which the formation of the single-phase zone is observed
- Diffusion couples with expected zig-zag behavior
- Diffusion couples with end-members lying on the same conode

Such a choice of diffusion couples was intended to provide experimental verification for a number of theoretical predictions present in the literature of subject [5,6,8,9], which in some cases remain still not verified, and in other are a source of controversies [26]. The design of the experiments, mainly the choice of compositions, benefited from the results of simulations, which allowed predicting the most basic features observed in the diffusion zones.

In the Fig. 2, the exemplary simulated profiles and diffusion paths for all three types of considered diffusion couples are presented, obtained with the use of both DICTRA and multi-multi models. Some of the differences between both these theoretical descriptions can be clearly seen:

The verification of these predictions is presented in the following sections. An important role in the multiphase diffusion can be assigned to the multiphase interfaces, which according to Morral et al. [10,12], can be classified as follows:

a) Type 0 boundary – occurs between alloys containing exactly the same types of phases. Its presence always results in the concentration jump along conode, which often leads to the zig-zag diffusion paths with or without horns. Furthermore, this type of boundary is stationary, meaning that the position of the Matano plane is independent of time. Type 0 boundaries occur only at the initial diffusion couple interface.
b) Type 1 boundary – in ternary systems such an interphase boundary occurs between single-phase and two-phase zones, e.g. $\gamma|\gamma+\beta$. Two cases of type 1 boundary can be distinguished: 1a, in which the single-phase zone is formed, and concentration jump occurs, and 1b, where the two-phase zone is formed, with no concentration jump being present.
c) Type 2 boundary – occurs when a single-phase zone transforms into another single-phase, with a jump of the diffusion path along the tie-line or when the two-phase zone transforms into another two-phase zone e.g. $\alpha+\gamma|\beta+\gamma$, with a diffusion path jump through tie-triangle on the phase diagram.
d) Type 3 boundary – occurs in ternary systems only when the diffusion path jumps through the tie-triangle, from its corner to the opposite two-phase field.

In the current study, only Type 0 and Type 1 boundaries are of relevance.

4.2. Experimental data

4.2.1. Diffusion with the single-phase zone formation

The possibility that diffusion in the two-phase zone can lead to the creation of a single-phase zone, when at least one of the initial compositions is placed close to a single-phase boundary (at the phase diagram), was predicted in numerous simulations [14,45,46]. Also, a similar behavior was observed during interdiffusion studies in other, relatively complex diffusion couples [25,34].

Both 1L|3R and 3L|3R diffusion couples presented in Figs. 3 and 4 exhibit a very good qualitative agreement with the mentioned postulates. SEM images of both samples reveal the formation of a single-phase γ-zone (between points 2 and 3 on the top of SEM image) with a thickness of 110 and 75 μm respectively. The part of the diffusion path corresponding to that zone follows the $\gamma|\gamma+\beta$-phase boundary. In both cases, the concentration jump on the left side of the γ-phase region (points 1, 2) is clearly visible, and this interphase boundary can be easily identified as a 1a-type. The right interphase boundary (point 3), does not exhibit the concentration jump and is not as sharp as in the previous case. However, the shape of the diffusion path is similar to the theoretically predicted one, and the expected concentration jump is relatively small. Therefore, it could have been smoothened by microstructure effects or hidden by measurement errors. As a result, this interphase boundary can also be considered as a 1a-type interphase boundary. All observed effects are in good agreement with theoretical predictions.

It can be seen that the terminal compositions of the couples are not completely equal to the assumed initial compositions of the alloys. These deviations are visible mainly in two-phase zones and are most likely caused by the limitation of the EDS method, as the signal is averaged from two phases characterized by different physical properties. In the case of the single-phase zones, no such problems were observed.

In both couples, the Matano plane position was calculated to overlie with the position of the main interphase boundary (point 1, 2). Therefore, it should not be surprising that the γ-zone grows at the expense of alloy 3R. In both couples, the markers indicate the presence of a single Kirkendall plane placed in γ-region. However, in the 3L|3R couple it is located close to the main interphase boundary (and Matano plane), while in 1L|3R couple it can be found 21 μm away. As a result, the 3L|3R couple is the only one in which the Frenkel porosity was observed. The pores are visible only within the γ-phase zone, close to the interphase boundary between γ-phase and 3R alloy (point 3).

The differences in the thickness of the γ-zones observed between both couples are worth noting. Starting with the experimental results of Nesbitt et al. [21] and ending with the recent simulation results [47], all authors claim that the thickness of the single-phase zone should increase with the increase of the given phase fraction in the initial composition. In other words, the closer the initial concentration points are placed to the single-phase boundary, the bigger the thickness of the forming single-phase zone should be. In our case, the opposite phenomenon is observed, which is rather surprising. Both the 1L and 3L alloys are placed on the same conode, therefore, the driving forces for the diffusion in both couples should be similar and cannot be held responsible for such behavior. Most likely, the justification can be

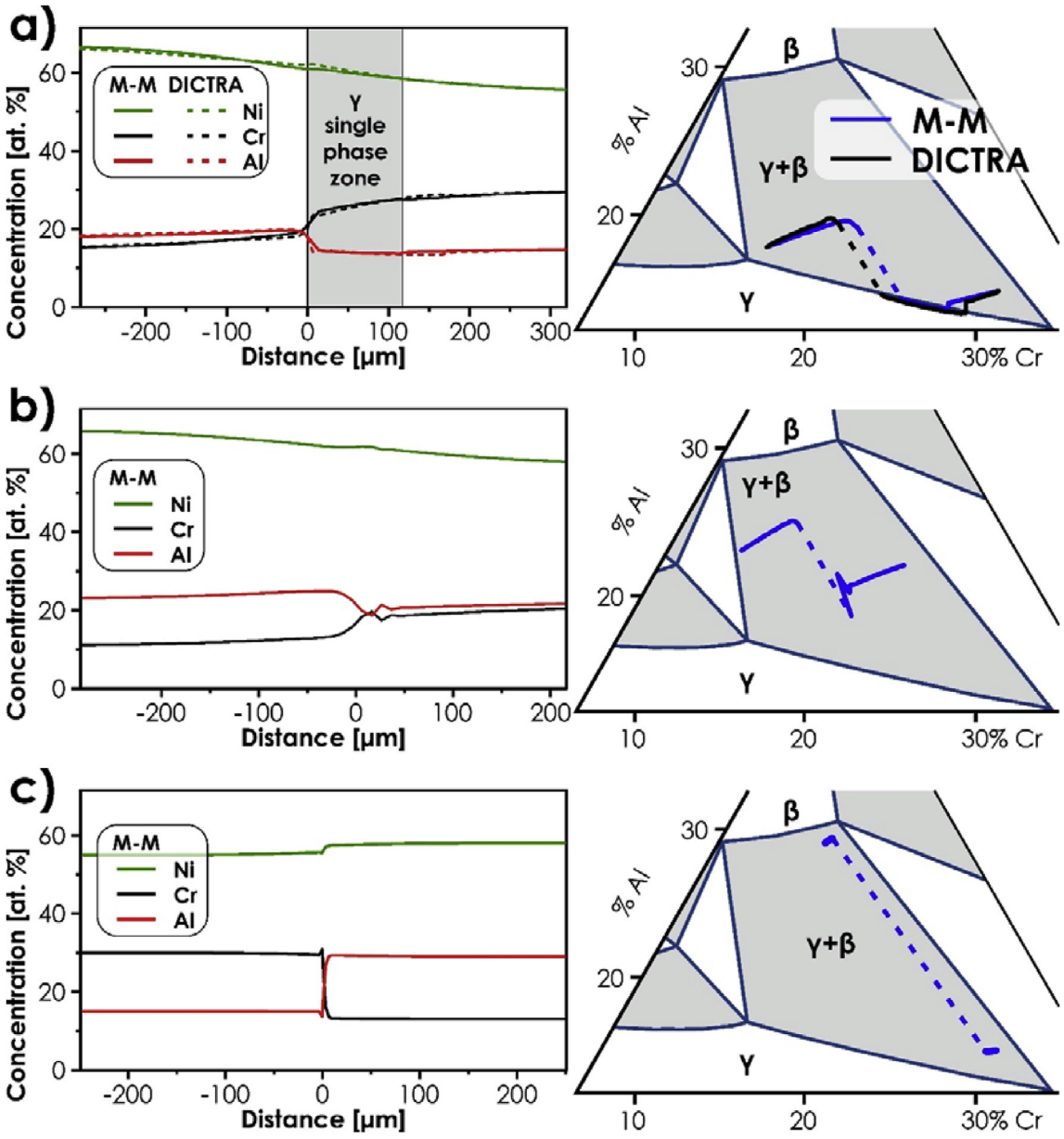

Fig. 2. Exemplary theoretical prediction obtained with the use of both DICTRA and M-M for diffusion couples of following types: a) diffusion couple in which the formation of the single-phase zone is observed; b) diffusion couple with expected zig-zag behavior; c) diffusion couples with end-members lying on the same conode.

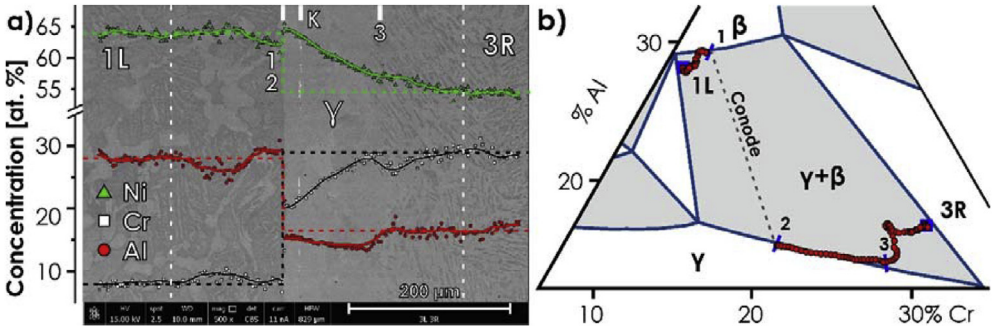

Fig. 3. Couple 1L|3R after annealing for 24 h at 1200 °C. a) SEM image with concentration profiles: scatter - the raw data, solid lines – smoothed by the Savitzki-Golay filter, dashed lines – the initial concentration distribution; b) diffusion path presented on the Ni-Cr-Al phase diagram. Symbols: K – position of the Kirkendall plane, points 1, 2, 3 – characteristic features observed within the diffusion zone, vertical dashed lines – indicative boundary of the interdiffusion zone, blue squares on the phase diagram – composition of the end-members. (For interpretation of the references to colour in this figure legend, the reader is referred to the Web version of this article.)

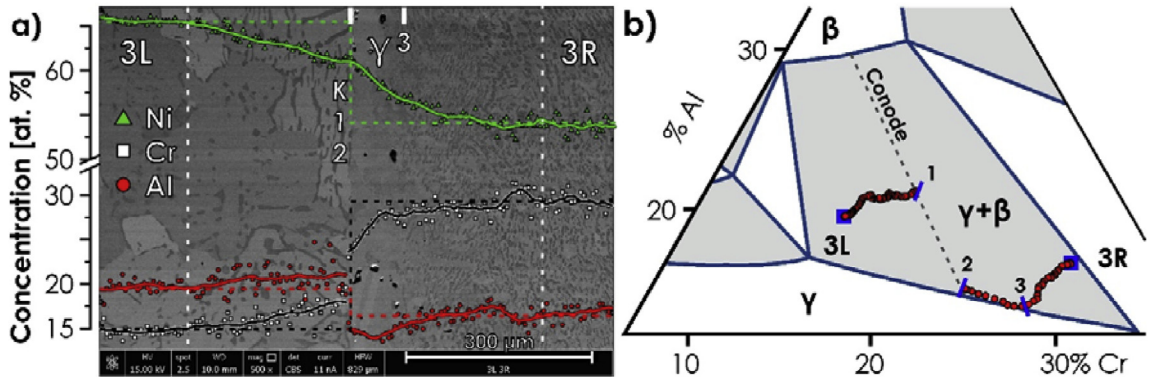

Fig. 4. Couple 3L|3R after annealing for 24 h at 1200 °C. a) SEM image with concentration profiles: scatter - the raw data, solid lines – smoothed by the Savitzki-Golay filter, dashed lines – the initial concentration distribution; b) diffusion path presented on the Ni-Cr-Al phase diagram. Symbols: K – position of the Kirkendall plane, points 1, 2, 3 – characteristic features observed within the diffusion zone, vertical dashed lines – indicative boundary of the interdiffusion zone, blue squares on the phase diagram – composition of the end-members. (For interpretation of the references to colour in this figure legend, the reader is referred to the Web version of this article.)

found in the differences between the diffusion coefficients in the γ and β phases. It is widely known that diffusion in β-phase occurs much faster than in γ [44,48]. Since the left end-member of the 1L|3R couple is characterized by a much higher content of the β phase, similar driving forces lead to a correspondingly faster diffusion rate, which in turn results in the formation of a wider γ region. Lack of a measurable shift between the Matano plane and the position of the interphase boundary, indicating a lack of accumulation, further suggests that the diffusion fluxes in the γ phase are enhanced. Since the values of the diffusion coefficients within γ phase have to be the same in both studied couples, in the case of the 1L|3R couple the system follows a diffusion path allowing enhancement of the chemical potential gradients and, as a result, increase of the diffusion fluxes. This can be observed as an elongated diffusion path through the γ zone, which is clearly visible in the comparison of Figs. 3b and 4b.

4.2.2. Zig-Zag diffusion

The 3L|1R couple shown in Fig. 5 exhibits almost model behavior of a typical two-phase diffusion couple with a very sharp, 0-type interphase (points 1, 2) boundary and zig-zag diffusion path with a clear concentration jump. The fluctuations visible on the concentration profiles, especially of chromium and aluminum in the left part of the couple, are likely caused by the structural effect (the structure of multiphase alloy is not fully uniform), and cannot be eliminated even by wide-line EDS analysis. Nevertheless, they do not affect our ability to interpret the results. The upper right part of the diffusion path (as visible on the phase diagram, Fig. 5b) is very short, and the concentration jump does not take place along the conode. Also, an outward-horn-like structure is visible close to the "1" point on the phase diagram. Both these effects can most likely be attributed to the limitations of the EDS method, as even relatively small errors of composition determination can generate effects visible on the phase diagram. Still, the typical "zig-zag" behavior of the diffusion path indicates that the mentioned difficulties should not be considered as relevant. No signs of the creation of a single-phase region are observed.

The markers indicate that the position of the Kirkendall plane overlays with the position of the 0-type interphase boundary. That is also true for the position of the Matano plane, therefore it can be said that the Kirkendall shift, in this case, is smaller than the measurement error.

The results obtained for the next 2L|2R diffusion couple are probably the most interesting and at the same time, the most difficult for interpretation. To eliminate the possibility of experimental error, this experiment was repeated, giving nearly identical results (the small differences between concentration profiles and diffusion paths are a natural consequence of the differences between two samples, see supplementary materials). The SEM image of the 2L|2R diffusion couple shown in Fig. 6 does not indicate the presence of a sharp 0-type interphase boundary, as the microstructure changes in an almost continuous way. Also, the concentration profile reveals a rapid change of concentration only in the area between points 1 and 3 (see Fig. 6a). In the middle of the

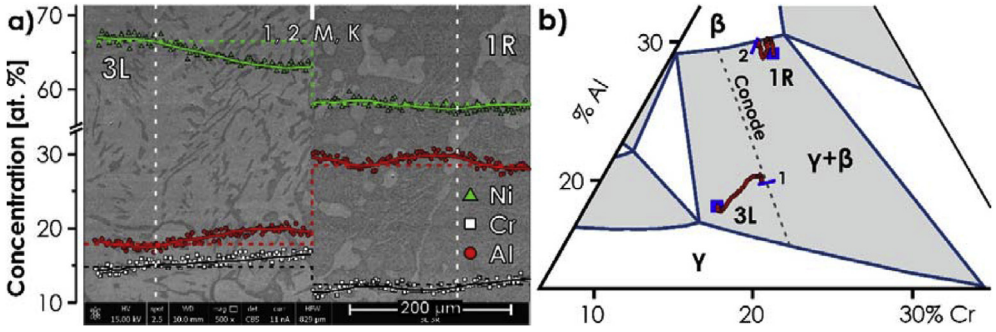

Fig. 5. Couple 3L|1R after annealing for 24 h at 1200 °C. a) SEM image with concentration profiles: scatter - the raw data, solid lines – smoothed by the Savitzki-Golay filter, dashed lines – the initial concentration distribution; b) diffusion path presented on the Ni-Cr-Al phase diagram. Symbols: M – position of the Matano plane, K – Kirkendall plane, points 1, 2 – characteristic features observed within the diffusion zone, vertical dashed lines – indicative boundary of the interdiffusion zone, blue squares on the phase diagram – composition of the end-members. (For interpretation of the references to colour in this figure legend, the reader is referred to the Web version of this article.)

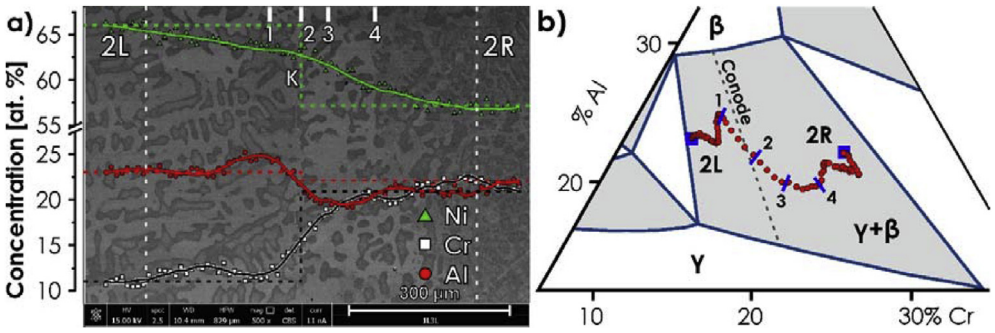

Fig. 6. Couple 2L|2R after annealing for 24 h at 1200 °C: a) SEM image with concentration profiles: scatter - the raw data, solid lines – smoothed by the Savitzki-Golay filter, dashed lines – the initial concentration distribution; b) diffusion path presented on the Ni-Cr-Al phase diagram. Symbols: K – position of the Kirkendall plane, points 1, 2, 3, 4 – characteristic features observed within the diffusion zone, vertical dashed lines – indicative boundary of the interdiffusion zone, blue squares on the phase diagram – composition of the end-members. (For interpretation of the references to colour in this figure legend, the reader is referred to the Web version of this article.)

diffusion couple cross-section, a lighter zone enriched in γ-phase is visible. However, the diffusion path correlated with this area (points 2-4) does not reach the single-phase region, contrary to what was observed by Sohn et al. [26]. On the other hand, the diffusion path presented in Fig. 6b is similar to the zig-zag diffusion path presented by Morral et al. [7] excluding, however, the lack of concentration jump on the interphase boundary. Additionally, the concentration change between points 1 and 2 does not occur along the conode. The obtained results do not confirm the existence of the "horns" either. The outward-horn-like structure visible near the 2L composition on the diffusion path (see Fig. 6b) was not observed in the repeated experiment and could have been a result of EDS errors.

Based on the position of the thorium dioxide markers shown in Fig. 7, the existence of two Kirkendall planes, spaced apart by the distance of about 20 μm, can be postulated. One of them can be assigned to the γ-phase and the second one to β-phase. It is a very strong argument for the assumption made by Danielewski et al. [18] that diffusion goes through both phases and two drift velocities should be considered, one for each phase. It should be noted that the Morral group also considered the movement of markers in a model two-phase diffusion couple [49]. However, they assumed that markers can move only in the matrix phase and the second phase is just an obstacle for them. Therefore, they did not obtain two Kirkendall planes, but only a single plane of markers with "marauders" remaining behind. The value of the calculated Matano plane position varied for different elements, due to the relatively low values of concentration gradients, and therefore, obtaining any useful information about the direction of markers movement was not possible.

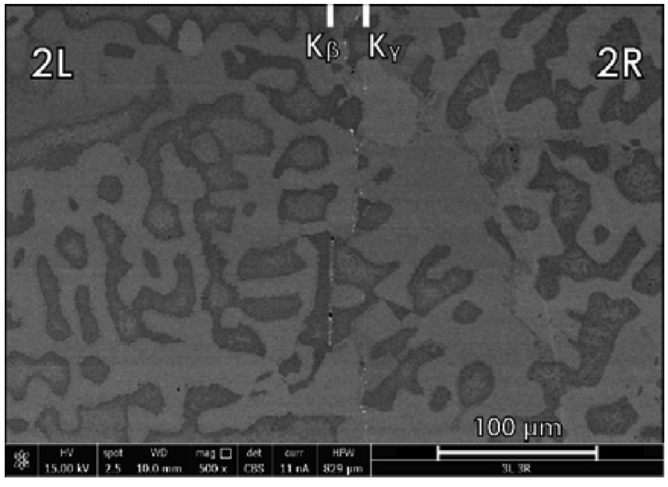

Fig. 7. Magnified micrography of the 2L|2R diffusion couple. Two separate Kirkendall planes, denoted as K_γ and K_β, are visible.

In light of the previous experiment and numerical simulation, the obtained results cannot be fully explained. The Phase-Field simulation performed by Pan et al. [50] allows suspecting that the γ-enriched zone is a transition structure, which should lead to obtaining a γ single-phase zone. However, this conclusion contradicts the second Kirkaldy theorem that the diffusion path (in the semi-infinite system) should be invariant of time [11].

4.2.3. Diffusion at conodes

Most of the models assume that the conodes connect the compositions having the same chemical potential. Therefore, there is no driving force in the system and consequently, interdiffusion does not occur. However, the very early paper published by Gusak et al. [51], suggests that the random walk of the atoms may result in a blur of concentrations along the conode.

To verify that assumption, two couples were prepared, namely 1L|3L and 1R|3R, in which initial concentrations are placed on the same conodes. The 24-h annealing did not yield decisive results (see supplementary materials). Therefore, the annealing was continued to reach the total time of 100 h. The results for the 1L|3L couple are presented in Fig. 8, together with the diffusion paths obtained for both "conode couples" after 100 h. The additional heating and quenching resulted in the change of microstructure. The observed fine microstructure allowed obtaining a very smooth concentration profile with sharp concentration jump at the phase boundary. Magnified SEM images show the diffusion zone of about 10 μm thickness. It may result from the small deviation of the used materials from the ideal conode compositions. Still, considering that in other diffusion couples the diffusion zone exceeded 100 μm, such a behavior can be deemed negligible. Therefore, it can be said that neither interdiffusion nor concentration blur occurs.

4.3. Simulations results, comparison of the models with the experimental data

The results of simulations for 1L|3R and 3R|3R diffusion couples are shown in Figs. 9 and 10. Under each figure in this section, the content of the γ-phase is presented as a function of the position within the diffusion zone, calculated based on the phase diagram for all concentration profiles. In the presented cases, the experimental rather than nominal compositions were used as end-members, as in this particular case even relatively small

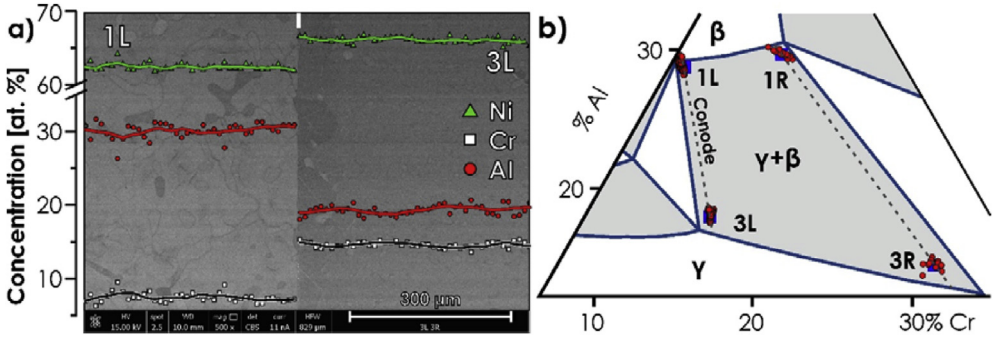

Fig. 8. Interdiffusion in couples with concentration of the end-members lying on the same conode, after annealing for 100 h at 1200 °C: a) SEM image for 1L|3L diffusion couple with concentration profiles: scatter - the raw data, solid lines – smoothed by the Savitzki-Golay filter; and b) diffusion paths for 1L|3L and 1R|3R couples presented on the Ni-Cr-Al phase diagram. Blue squares denote the composition of the end-members of both couples. (For interpretation of the references to colour in this figure legend, the reader is referred to the Web version of this article.)

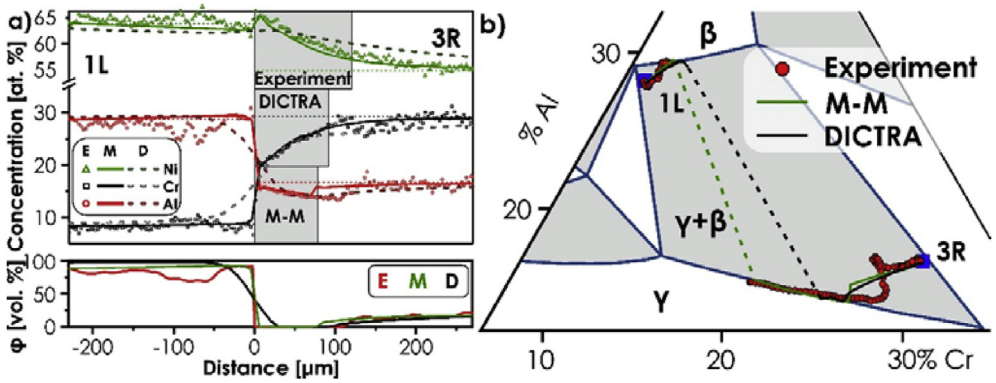

Fig. 9. The comparison of simulations results obtained by the use of DICTRA (D) and multi-multi (M) methods with the experimental data (E) for the 1L|3R diffusion couple. a) concentration profiles with marked single-phase phase zones (grey areas) obtained by experiment, DICTRA, and multi-multi model. The horizontal dashed lines indicate the values of initial concentration. The calculated content of β-phase is presented below; b) diffusion paths placed on the phase diagram. The concentration jumps on the simulated diffusion paths are marked by the dashed lines. Blue squares denote the composition of the end-members. (For interpretation of the references to colour in this figure legend, the reader is referred to the Web version of this article.)

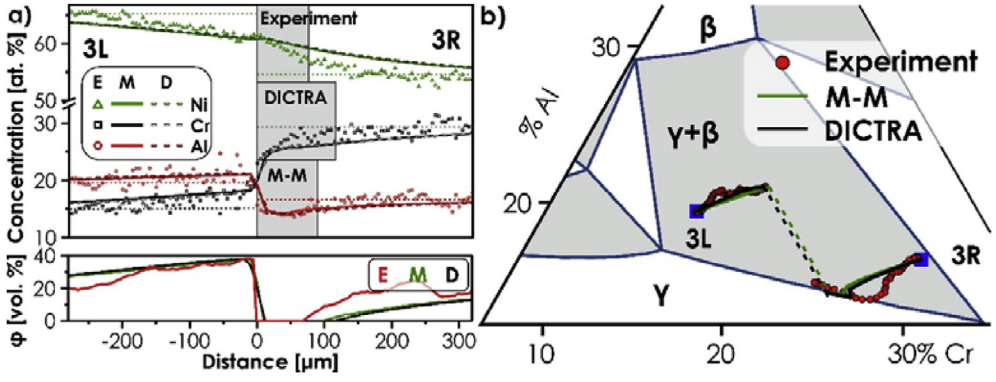

Fig. 10. The comparison of simulations results obtained by the use of DICTRA (D) and multi-multi (M) methods with the experimental data (E) for the 3L|3R diffusion couple. a) concentration profiles with marked single-phase phase zones (grey areas) obtained by experiment, DICTRA and multi-multi model. The horizontal dashed lines indicate the values of initial concentration. The calculated content of β-phase is presented below; b) diffusion paths placed on the phase diagram. The concentration jumps on the simulated diffusion paths are marked by the dashed lines. Blue squares denote the composition of the end-members. (For interpretation of the references to colour in this figure legend, the reader is referred to the Web version of this article.)

deviations of the compositions may affect the shape of the diffusion paths. The concentration profiles and diffusion paths obtained by both models predict the existence of the single-phase γ-zone and are in a qualitative agreement with the experiment, with a slightly better quality of fitting for the multi-multi model. It is especially visible for the diffusion paths of couple 1L|3R (Fig. 9b). While the diffusion path predicted by the multi-multi model is in nearly full agreement with the experiment, the one predicted by DICTRA exhibits concentration jump along a completely different conode. On the other hand, for the couple 3L|3R, both models yield nearly identical results and only small, negligible differences can be observed between the diffusion paths.

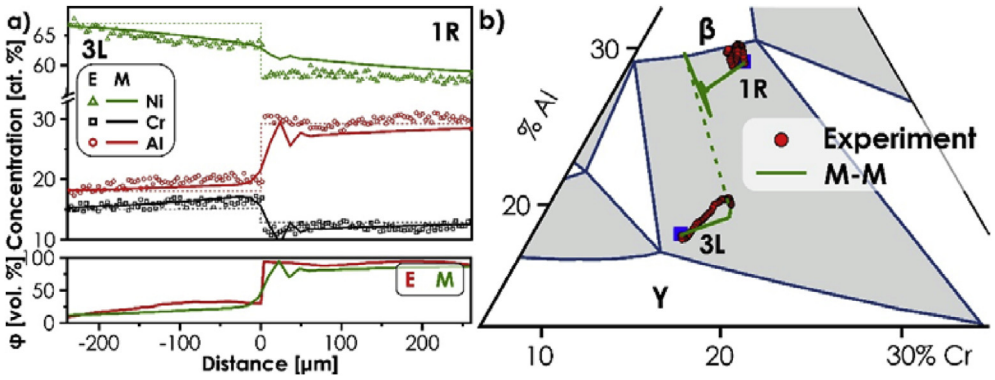

Fig. 11. The comparison of simulations results obtained by multi-multi (M) methods with the experimental data (E) for the 3L|1R diffusion couple. a) concentration profiles, the calculated content of β-phase is presented below. The horizontal dashed lines indicate the values of initial concentration; b) diffusion paths placed on the phase diagram. The concentration jumps on the simulated diffusion path is marked by the dashed lines. Blue squares denote the composition of the end-members. (For interpretation of the references to colour in this figure legend, the reader is referred to the Web version of this article.)

The thickness of the single-phase, γ-zone predicted by DICTRA is in both cases slightly higher than the one obtained by multi-multi model. However, both are in similar proximity to the γ-zone thickness observed in the experiment. As for the diffusion paths, the fragments corresponding to the single-phase γ-zone are significantly shorter than experimentally measured ones, especially in the case of DICTRA results for the 1L|3R diffusion couple.

For the couple 1L|3R, the multi-multi model predicted a sharp concentration jump, which is in good agreement with the experiment. On the other hand, the DICTRA simulations predicted a much less steep change. Also, the values of concentration for the right side of the concentration-position plot differ from the experimental concentrations. It results from the fact that the diffusion zone predicted by DICTRA is much wider. It should be mentioned that the total length of simulated couples was much higher than the part presented on the graphs.

Similar behavior can be observed for the 3L|3R couple. However, in this case, both models yield nearly identical results in terms of concentration profiles.

In the case of the couples with a two-phase zone only, namely 3L|1R and the 2L|2R, we were not able to obtain any meaningful results using DICTRA software, with either the system behaving like a single-phase solid solution or the calculations being terminated due to the presence of numerical errors. In our opinion, the most likely reason for such behavior lies in the high content of β-phase, as according to Engström et al. [14] the DICTRA approach of continuous matrix and precipitates of the second phase provides reasonable results when the volume of the second phase does not exceed 40%. This assumption is not fulfilled for both 3L|1R and 2L|2R couples, where the amount of the β-phase exceeds this value.

As a result, the following simulations were performed using the multi-multi model only. The results of the simulation for the 3L|1R couple are shown in Fig. 11. The lower left part of the diffusion path is in good agreement with the experiment. However, the jump of concentration does not terminate close to the end of the experimentally measured upper right part. The gap between experimental and simulated concentration profiles for the right side of the concentration position-plot is clearly visible also on the diffusion path. It can derive from the specifics of numerical simulation, in which the concentration jump is sharp and occurs along one specific conode. The experimental concentration jump does not and this deviation can be caused by the typical uncertainty od EDS methods, the two-phase microstructural noise, and the limitation of the applied model as well. The observed undulation of the simulated diffusion path can be attributed strictly to the numerical errors, which could be minimized but not completely removed by a change of simulation parameters such as time step, change of the calculation grid, etc. It should be noted that similar numerical artifacts can also be observed for calculations with the use of the DICTRA model, and most probably can be attributed to the non-continuity of concentration functions at the interphase boundary. In this couple, the phase contents for both experimental and theoretical concentrations remain in a good agreement.

As expected, the simulation for the 2L|2R couple (See Fig. 12) resulted in a zig-zag diffusion path, which is not in a full agreement with the experimental results. What is worth noting, in this case by far the biggest discrepancies between the phase contents calculated based on the experimental concentrations and simulated ones occur. The diffusion path obtained in simulation possesses a characteristic concentration jump along a conode, while in the case of experimental one, a continuous transition between terminal compositions is observed. Still, the general directions of both simulated and measured diffusion paths are similar. Nevertheless, despite the mentioned differences, the comparison of simulated and experimental concentration profiles looks surprisingly good, except for the lack of concentration jump. To sum up, despite the non-typical behavior of this specific diffusion couple, the multi-multi model allows a reasonably good prediction of the observed phenomena. Still, the results strongly suggest that some of the measured effects are outside available theoretical knowledge. Taking into account the results reported by Sohn et al. [26], it can be said that the complexity of the interdiffusion phenomenon in the two-phase zone may be much higher than previously expected.

5. Conclusions

In the presented study, the two-phase diffusion couples from the Ni-Cr-Al ternary systems were studied, allowing for the first time obtaining good quality data concerning the diffusion in two-phase zones. The main conclusions are as follows:

- The experimental investigation of interdiffusion in two-phase γ+β zone of Ni-Cr-Al system allowed verification of multiple theoretical assumptions formulated in the past, such as:
  - I) existence of zig-zag diffusion paths;
  - II) single-phase zone formation;
  - III) no interdiffusion between compositions lying on the same conode;
  - IV) the possibility of the existence of two different Kirkendall planes.

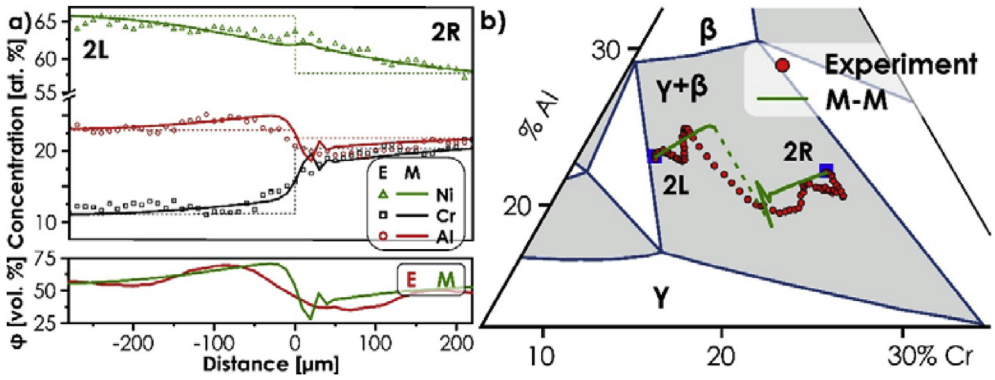

Fig. 12. The comparison of simulations results obtained by multi-multi (M) methods with the experimental data (E) for the 2L|2R diffusion couple. a) concentration profiles b) diffusion paths placed on the phase diagram, the calculated content of β-phase is presented below. The horizontal dashed lines indicate the values of initial concentration. The concentration jumps on the simulated diffusion path is marked by the dashed lines. Blue squares denote the composition of the end-members. (For interpretation of the references to colour in this figure legend, the reader is referred to the Web version of this article.)

- The application of the innovative WL-EDS analysis, characterized by much better accuracy and space resolution than previously applied methods, allows for interpretation of the data from multiphase zones on the qualitative level. However, the non-uniform phase composition and microstructure hamper the quantitative data interpretation and may have led to significant deviations from the theoretical behavior. Despite that, the presented approach offers a unique chance to study and to understand the interdiffusion in two-phase systems on both experimental and theoretical level and can be further improved e.g. through optimization of the WL-EDS method parameters.
- The application of both DICTRA and multi-multi methods allowed for generally correct description of the interdiffusion phenomena. Considering the differences between the models, it can be therefore stated that one of the key features to successful interpretation of the diffusion data in multiphase systems is the assumption of diffusion occurring in all phases present in the diffusion zone.
- Further studies should concentrate on incorporating the full thermodynamics of the studied systems, combined with the extension of currently available tracer diffusion data in different crystallographic phases. Only then will it be possible to provide a full, detailed description of the interdiffusion process.

Author contributions section

M. Zajusz: General idea of the research; numerical simulation; data processing, data interpretation; writing; supervision.

M. Jawańska: Experimental parts; numerical simulation; data processing; data interpretation; writing.

J. Dąbrowa: Data processing, data interpretation, writing, supervision.

K. Berent: Experimental parts of the project.

M. Danielewski: data interpretation, writing; supervision.

Declaration of competing interest

The authors declare that they have no known competing financial interests or personal relationships that could have appeared to influence the work reported in this paper.

Acknowledgments

The DICTRA computations were performed thanks to the kindness of Access e.V. in Aachen (Germany) during an internship in April 2019.

This work is supported by a National Science Center (Poland) decision no. DEC- 2017/25/B/ST8/02549.

Appendix A. Supplementary data

Supplementary data to this article can be found online at https://doi.org/10.1016/j.jallcom.2020.155513.

References

[1] G.W. Roper, D.P. Whittle, Interdiffusion in two-phase thernary solid systems, Mater. Sci. 148 (1981) 148–153.
[2] W.D. Hopfe, J.E. Morral, Zigzag diffusion paths in multiphase diffusion couples, Acta Metall. Mater. 42 (1994) 3887–3894.
[3] A. Engström, L. Höglund, J. Ågren, Computer simulation of diffusion in multiphase systems, Metal, Mater. Trans. 25 (1994) 1127–1134.
[4] H. Yang, J.E. Morral, Y. Wang, On diffusion paths with “horns” and the formation of single phase layers in multiphase diffusion couples, Acta Mater. 53 (2005) 3775–3781.
[5] K. Wu, J.E. Morral, Y. Wang, Horns on diffusion paths in multiphase diffusion couples, Acta Mater. 54 (2006) 5501–5507.
[6] M. Schwind, T. Helander, J. Agren, On zigzag shaped diffusion paths in multiphase diffusion couples, Scripta Mater. 44 (2001) 415–421.
[7] J.E. Morral, X. Pan, N. Zhou, H. Larsson, Y. Wang, Singularities in multiphase diffusion couples, Scripta Mater. 58 (2008) 3854–3861.
[8] C.W. Yeung, W.D. Hopfe, J.E. Morral, A.D. Romig, Interdiffusion in high-temperature 2-phase, Ni-Cr-Al coating alloys, Mater. Sci. Forum 163–165 (1994) 189–194.
[9] C. Jin, J.E. Morral, Microstructures from Ni-Cr-Al diffusion couples illustrating "three types of boundaries, Scripta Mater. 37 (1997) 621–626.
[10] J.E. Morral, C. Jin, A. Engstrom, J. Agren, Three typesof planar boundary in multiphase diffusion couples, Scripta Mater. 34 (1996) 1661–1666.
[11] J.S. Kirkaldy, L.C. Brown, Diffusion behaviour in ternary, multiphase systems, Can. Matall. Q. 2 (1963) 89–115.
[12] J.E. Morral, Diffusion path theorems for ternary diffusion couples, metal, Mater. Trans. 43A (2012) 3462–3470.
[13] J.O. Andersson, L. Höglund, B. Jönsson, J. Ågren, Computer simulation of multicomponent diffusional transformations in steel, in: G.R. Purdy (Ed.), Fundamentals and Applications of Ternary Diffusion, Pergamon, Oxford, 1990, pp. 153–163.
[14] A. Engstrom, J.E. Morral, J. Agren, Computer simulations of Ni-Cr-Al multiphase diffusion couples, Acta Mater. 45 (1997) 1189–1199.
[15] K. Wu, N. Zhou, X. Pan, J.E. Morral, Y. Wang, Multiphase Ni-Cr-Al diffusion couples: a comparison of phase field simulations with experimental data, Acta Mater. 56 (2008) 3854–3861.
[16] X.Q. Ke, J.E. Morral, Y. Wang, Type n boundaries in n-component diffusion couples, Acta Mater. 61 (2013) 2339–2347.
[17] N. Ta, L. Zhang, Y. Du, A trial to design γ/γ′ bond coat in Ni–Al–Cr mode TBCs aided by phase-field simulation, Coatings 8 (2018) 421–440.
[18] M. Danielewski, B. Wierzba, K. Tkacz-Śmiech, A. Nowotnik, B. Bożek, J. Sieniawski, Bi-velocity model of mass transport in two-phase zone of ternary system, Philos. Mag. A 93 (2013) 2044–2056.
[19] S.R. Le Vine, Reaction diffusion in the NiCrAl and CoCrAl systems, Metal, Mater. Trans. 9 (1978) 1237–1250.

[20] L.A. Carol, A Study of Interdiffusion in β+y/y+y' Ni-Cr-Al Alloys a T 1200 °C, Michigan Technological University, Houngton, Michigan, 1985.
[21] J.A. Nesbitt, R.W. Heckel, Interdiffusion in Ni-rich, Ni-Cr-Al alloys at 1100 and 1200 C: Part I. Diffusion paths and microstructures, Metal. Trans. A 18A (1987) 2061–2073.
[22] J.A. Nesbitt, R.W. Heckel, Interdiffusion in Ni-rich, Ni-Cr-Al alloys at 1100 and 1200 C: Part II. Diffusion coefficients and predicted concentration profiles, Metal. Trans. A 18A (1987) 2075–2086.
[23] S.M. Merchant, M.R. Notis, J.I. Goldstein, Interface stability in the Ni-Cr-Al system: Part I. Morphological stability of β-γ diffusion couple interfaces at 1150°C metal, OR Trans. 21 (1990) 1901–1910.
[24] S.M. Merchant, M.R. Notis, J.I. Goldstein, Interface stability in the Ni-Cr-Al system: Part II. Morphological stability of β-Ni50Al vs γ-Ni40Cr diffusion couple interfaces at 1150°C, Metal. Trans. A 21 (1990) 1911–1919.
[25] X. Qiao, in: M.S. Thesis., University of Connecticut, 1998.
[26] Y.H. Sohn, A. Puccio, M.A. Dayananda, Interdiffusion structures and paths for multiphase Fe-Ni-Al diffusion couples at 1000 C, metal, Mater. Trans. 36A (2005) 2361–2370.
[27] Z.W. Yang, J. Lian, J. Wang, X.Q. Cai, Y. Wang, D.P. Wang, Z.M. Wang, Y.C. Liu, Diffusion bonding of Ni3Al-based alloy using a Ni interlayer, J. Alloys Compd. 819 (2020) 153324.
[28] T. Buasri, K. Goto, M. Tahara, H. Hosoda, Phase reaction and diffusion behavior between AuTi and CoTi intermetallic compounds, Mater. Trans. 60 (2019) 631–635.
[29] C.M. Eastman, J.-C. Zhao, Phase equilibria and diffusion in the Ni-Cr-Pt system at 1200 °C, J. Phase Equilibria Diffus. 40 (2019) 542–552.
[30] M.R. McGregor, M.E. Hancock, L. Pallett, W.J. Clegg, Examination of Ni-based superalloy/intermetallic diffusion couples containing multiphase regions, Intermetallics 113 (2019) 106559.
[31] B. Wierzba, W.J. Nowak, The diffusion path model in a ternary multiphase system, Physica A 509 (2018) 265–274.
[32] B. Wierzba, W.J. Nowak, D. Serafin, The sequence of the phase growth during diffusion in Ti-based systems, High Temp. Mater. Process. 38 (2019) 151–157.
[33] D. Serafin, W.J. Nowak, B. Wierzba, The calculation of the diffusion coefficients in ternary multiphase Ti-NiAl system, Comput. Mater. Sci. 165 (2019) 1–6.
[34] K. Tkacz-Śmiech, M. Danielewski, B. Bożek, K. Berent, D. Zientara, M. Zajusz, Diffusive ineraction between Ni-Cr-Al alloys, Metall. Mater. Trans. 48A (2017) 2633–2642.
[35] J.O. Andersson, T. Helander, L.H. Hoglund, P.F. Shi, B. Sundman, THERMO-CALC & DICTRA, computational tools for materials science, Calphad 26 (2002) 273–312.
[36] K. Hashimoto, T. Abe, Y. Sawada, TDB-file for the thermodynamic assessment of the Al-Cr-Ni system, in: National Institute for Materials Science, 2014.
[37] S. Hayashi, D. Kudo, R. Nagashima, H. Utsumi, Effect of Cu on oxidation behaviour of FCC Fe-Ni-Cr-Al and Ni-Cr-Al based alloys, Corrosion Sci. 163 (2020) 108273.
[38] T.-H. Kang, K.-S. Kim, M.-H. Park, K.-A. Lee, High temperature random stack creep property of Ni-Cr-Al based powder porous metal manufactured with powder sintering process, Arch. Metall. Mater. 64 (2019) 513–518.
[39] Z. Mao, C. Booth-Morrison, C.K. Sudbrack, R.D. Noebe, D.N. Seidman, Interfacial free energies, nucleation, and precipitate morphologies in Ni-Al-Cr alloys: calculations and atom-probe tomographic experiments, Acta Mater. 166 (2019) 702–714.
[40] S.V. Raju, B.K. Godwal, A.K. Singh, R. Jeanloz, S.K. Saxena, High-pressure strengths of Ni3Al and Ni-Al-Cr, J. Alloys Compd. 741 (2018) 642–647.
[41] A.M. Gusak, Diffusion-controled Solid State Reactions, Wiley-VCH, 2010.
[42] A. Savitzky, M.J.E. Golay, Smoothing and differentiation of data by simplified least squares procedures, Anal. Chem. 36 (1964) 1627–1639.
[43] K. Wu, J.E. Morral, Y. Wang, A phase field study of microstructural changes due to the Kirkendall effect in two-phase diffusion couples, Acta Mater. 49 (2001) 3401–3408.
[44] C.E. Campbell, Assessment of the diffusion mobilites in the γ′ and B2 phases in the Ni-Al-Cr system, Acta Mater. 56 (2008) 4277–4290.
[45] W.J. Boettinger, S.R. Coriell, C.E. Campbell, G.B. McFadden, On the properties of alpha/alpha+beta ternary diffusion couples, Acta Mater. 48 (2000) 481–492.
[46] M. Danielewski, A.M. Gusak, B. Bożek, M. Zajusz, Model of diffusive interaction between two-phase Alloys with explicit fine-tuning of the morphology evolution, Acta Mater. 108 (2016) 68–84.
[47] X.Q. Ke, J.E. Morral, Y. Wang, Fundamentals of interdiffusion microstructure maps for dual-alloy systems, Acta Mater. 76 (2014) 463–471.
[48] H. Chen, J.E. Morral, Variation of the effective diffusivity in two-phase regions, Acta Mater. 47 (1999) 1175–1180.
[49] K. Wu, J.E. Morral, Y. Wang, Movement of Kirkendall markers, second phase particles and the Type 0 boundary in two-phase diffusion couple simulations, Acta Mater. 52 (2004) 1917–1925.
[50] X. Pan, N. Zhou, J.E. Morral, Y. Wang, Microstructural stability in multi-alloy systems: nanostructured two-phase, dual alloy multilayers, Acta Mater. 58 (2010) 4149–4159.
[51] A.M. Gusak, Y.A. Lyashenko, Unique features encountered in the solution of equations for the diffusion transfer of mass in the two-phase zone of a triple system, J. Eng. Phys. 59 (1991) 1044–1049.